Proceedings of the Seventh International Conference on
Railway Technology: Research, Development and Maintenance
Edited by: J. Pombo
Civil-Comp Conferences, Volume 15, Paper 9.8
Civil-Comp Press, Edinburgh, United Kingdom, 2026
ISSN: 2753-3239, doi: 10.4203/ccc.15.9.8

Leakage Simulation of Train Brake Pipeline Threaded Joints Based on Contact-Pressure Connectivity Analysis

H. Zhou, J. Zuo, Y. Pan and J. Ding

College of Transportation, Tongji University, Shanghai, China

Abstract

To address the gas leakage problem of threaded pipe joints in a train brake pipeline under low-temperature service conditions, a three-dimensional finite element contact model of a conventional threaded pipe joint was established in this study. Since the gap value directly obtained from finite element analysis is insufficient to accurately characterize the actual leakage opening and the risk of through-leakage paths, a leakage channel identification method based on a contact-pressure connectivity criterion was proposed. The results show that, with increasing tightening torque, the high-pressure regions on the threaded contact surface gradually expand and form locally continuous compressed zones, which effectively weaken the connectivity of low-pressure regions. Under low-torque conditions, the low-pressure regions are more likely to form continuous leakage paths in both the circumferential and axial directions. Compared with the room-temperature condition, low temperature causes redistribution of the contact state, enlarges the candidate leakage regions, and significantly increases the number of leakage elements, the equivalent leakage area, and the equivalent flow index. The proposed criterion overcomes the limitations of a single gap-based criterion, which is sensitive to local numerical values and cannot effectively determine the connectivity of leakage paths. The method provides a reference for leakage risk assessment and assembly parameter optimization of conventional threaded pipe joints under low-temperature conditions.

Keywords: threaded pipe joint, contact pressure, connectivity criterion, leakage channel, low temperature, finite element analysis.

1 Introduction

The airtightness of brake pipelines is directly related to braking response, braking efficiency, and operational safety of railway vehicles. During service, brake pipeline joints are subjected to internal pressure, vibration, impact, temperature variation, and assembly loads, which may degrade the sealing interface and induce gas leakage. In low-temperature winter environments, air leakage has frequently occurred at the main brake pipe and joint seals of certain train brake systems, indicating that the sealing reliability of existing pipeline connection structures may be insufficient under severe service conditions.

Conventional threaded pipe joints are still used in train brake pipeline connections. Unlike ferrule fittings or conical sealing structures with continuous sealing surfaces, the sealing performance of threaded joints depends strongly on the real contact state of the thread pair, the tightening torque, the distribution of locally compacted regions, and the blockage of micro-leakage paths. Owing to the helical geometry of threads, the contact pressure on the interface is usually non-uniform and affected by geometric deviation, contact nonlinearity, friction, and material deformation. Therefore, even if high contact pressure exists in some local regions, continuous low-pressure or insufficiently compacted zones may still form potential leakage paths from the high-pressure side to the low-pressure side. As a result, leakage risk cannot be evaluated only by local gap values or local contact pressure, but should be assessed together with the spatial distribution and connectivity of low-pressure regions.

Existing studies on threaded connections and metallic sealing structures have mainly focused on contact pressure distribution, effective sealing width, leakage rate prediction, and structural parameter optimization. For premium threaded connections used in tubing and casing strings, finite element models have been developed to investigate the effects of make-up torque, axial load, bending load, internal pressure, and temperature on sealing performance [1–4]. For pipe connectors and metallic sealing structures, previous studies have evaluated sealing performance based on contact pressure, critical sealing pressure, effective sealing width, leakage rate models, and thermo-mechanical coupling analysis [5–10]. In addition, leakage mechanisms have been studied from the perspectives of rough surface contact, percolation theory, micro-leakage channels, and multi-scale contact analysis [11–14]. These studies provide useful references for sealing performance evaluation; however, most of them focus on premium threaded connections, ferrule joints, conical sealing structures, or rough-surface leakage models. Research on leakage channel identification for conventional threaded pipe joints in train brake pipelines under low-temperature conditions remains limited.

To address this issue, this study establishes a three-dimensional finite element contact model of a conventional threaded pipe joint under different tightening torques and temperature conditions. Considering that the gap value directly obtained from finite element analysis cannot accurately represent the actual leakage opening or the connectivity of leakage paths, a leakage channel identification method based on a contact-pressure connectivity criterion is proposed. In this method, regions with contact pressure higher than a critical value are regarded as effectively compacted regions, while continuous low-pressure or insufficiently compacted regions connecting the inner and outer sides of the interface are identified as potential through-leakage channels. Furthermore, the equivalent gap height, number of leakage elements, effective leakage area, and equivalent flow index are introduced to semi-quantitatively evaluate the leakage risk under different torque and temperature conditions. The proposed method provides a reference for low-temperature leakage risk assessment and assembly parameter optimization of conventional threaded pipe joints in train brake pipeline systems.

2 Finite Element Model and Loading Conditions

To investigate the sealing performance of conventional threaded pipe joints under varying tightening torques and low-temperature service conditions, a three-dimensional finite element (FE) contact model of the threaded joint was developed. Potential leakage paths were identified based on contact pressure, contact gap, and the connectivity of low-pressure regions. The FE model construction involved geometry correction, material property definition, mesh generation, contact definition, and application of loads and boundary conditions. This section focuses on the FE modeling methodology and the definition of different service conditions, providing the computational basis for subsequent leakage path identification and sealing performance evaluation.

2.1 Geometry Model

The conventional threaded pipe joint consists of a central joint body and threaded pipe segments on both sides.The 3D model was derived from the brake mainline joint of a specific train, and was simplified and processed in CATIA to remove small chamfers, holes, and redundant features that could complicate meshing or induce local stress concentrations, while preserving the main contact and load-bearing geometry.

During 3D geometry correction, the original design model underwent topology optimization and tolerance adjustments to better represent the post-assembly contact state. Regions prone to local stress concentration, mesh distortion, or abnormal contact were locally modified to maintain geometric continuity in the thread contact and sealing regions. The corrected model preserves the main structural features of the threaded joint while enhancing computational operability and convergence stability for contact analysis.

2.2 Material Properties

The threaded pipe joint material was defined as ZG08Cr18Ni9, while the stainless-steel ferrule, nut, and joint body were modeled using X6CrNiMoTi17-12-2 and X5CrNi18-10. Material properties included elastic modulus, Poisson’s ratio, density, yield strength, ultimate tensile strength, thermal expansion coefficient, thermal conductivity, and specific heat. Detailed parameters are listed in Tables 1 and 2.

Property	Value	Property	Value
Elastic modulus (GPa)	195	Yield strength (MPa)	196
Poisson's ratio	0.29	Ultimate tensile strength (MPa)	449
Thermal expansion coefficient ($\times10^{-6}$/°C)	16	Density (kg/m³)	7900
Thermal conductivity (W/(m·°C))	15	Specific heat (J/(kg·°C))	500

Table 1: Material Properties of ZG08Cr18Ni9 for Sealing Pipe-Joint.

Property	Value	Property	Value
Elastic modulus (GPa)	195–200	Yield strength (MPa)	205
Poisson's ratio	0.29–0.30	Ultimate tensile strength (MPa)	515
Thermal expansion coefficient ($\times10^{-6}$/°C)	16–17	Density (kg/m³)	7980–8030
Thermal conductivity (W/(m·°C))	14–16	Specific heat (J/(kg·°C))	500–520

Table 2: Material Properties of X6CrNiMoTi17-12-2 for Sealing Pipe-Joint.

All materials were modeled as isotropic elastic-plastic. Considering potential local contact pressure redistribution under tightening and low-temperature effects, material nonlinearity, contact nonlinearity, and geometric nonlinearity were incorporated to improve simulation fidelity.

2.3 Mesh Generation

The finite element mesh was generated using HyperMesh. Due to the geometric complexity of thread contact regions and the sensitivity of contact pressure, gap, and penetration results to mesh quality, local mesh refinement was applied to critical contact areas. The model employed C3D8R eight-node linear reduced integration solid elements, which are suitable for 3D contact analysis with good computational efficiency and convergence stability, meeting the requirements for thermo-mechanical contact calculations. The meshing results are shown in Figure 1.

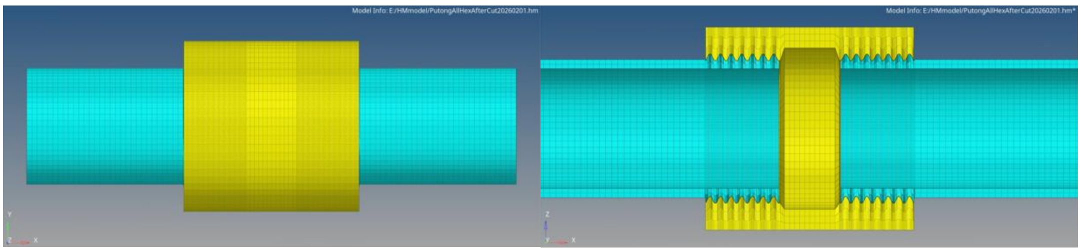

Figure 1: Mesh of the Threaded Joint Geometry (including cross-section view).

After meshing, the model comprised approximately 51,360 elements and 73,080 nodes. The mesh in thread contact and sealing regions was regular and sufficiently dense to support contact pressure distribution, contact gap evaluation, and leakage path identification.

2.4 Contact Definition

The sealing performance depends primarily on the compaction of the thread contact surfaces and the connectivity of low-pressure zones. Frictional contact was defined between the threaded pipe segments and the central joint, with a friction coefficient of 0.1.

2.5 Boundary Conditions and Load Application

To simulate assembly and service loading conditions, the central joint body was fixed, and loads were applied to the ends of the pipe segments. Loads considered included tightening torque, internal pipe pressure, temperature variation, and vertical loads. Internal pressure was 600 kPa, applied to the inner wall to represent normal braking pressure. Temperature conditions included 20 °C (ambient) and −40 °C (winter low-temperature scenario). Vertical loads of 500 N were applied to simulate vibration, impact, or eccentric loads during train operation.

An equivalent rotation method was adopted to simulate tightening, as directly applying torque can cause convergence difficulties. Specified rotation angles were applied to the pipe ends, generating corresponding tightening torque through remote reaction moments (Table 3). This geometric rotation approach more directly reflects thread rotation during tightening and forms the basis for leakage path identification.

Torque (N·m)	Thread Rotation (°)	Pressure (Pa)	Temperature (°C)	Vertical Load (N)
40	1	600,000	20 / −40	500
70	1.4	600,000	20 / −40	500
100	1.8	600,000	20 / −40	500
130	2.2	600,000	20 / −40	500
160	2.6	600,000	20 / −40	500
190	3	600,000	20 / −40	500

Table 3: Loading Conditions Using Geometric Rotation Method.

2.6 Load Steps

A stepwise loading procedure was employed to improve convergence and distinguish the effects of assembly, thermal, and external loads (Table 4).

Step	Time (s)	Applied Load	Purpose
1	0–0.001	Equivalent pre-tension or geometric rotation	Simulate assembly tightening and form initial contact pressure
2	0.001–0.002	Internal pressure and temperature change	Simulate operating pressure and low-temperature effects
3	0.002–0.003	Vertical load	Simulate vibration, impact, or eccentric loads during operation

Table 4: Load Step Definitions for Finite Element Analysis.

The first load step establishes initial compaction of the thread contact surfaces. The second step applies internal pressure and temperature change to evaluate opening forces and thermal contraction effects. The third step simulates operational disturbances to assess their influence on leakage path connectivity.

2.7 Condition Combinations and Result Extraction

Multiple loading conditions were simulated with tightening torques of 40, 70, 100, 130, 160, and 190 N·m, temperatures of 20 °C and −40 °C, internal pressure of 600 kPa, and vertical load of 500 N. FE results were extracted for contact status, contact gap, penetration, and contact pressure. Contact pressure was used to identify effectively compacted regions; the gap was used to estimate equivalent leakage openings; status and penetration were used to verify the contact condition (Figure 2 presents the pressure results, 190N·m). The results were post-processed in MATLAB to identify low-pressure regions forming continuous leakage paths and to calculate the number of leakage elements, equivalent gap height, effective leakage area, and equivalent flow indices.

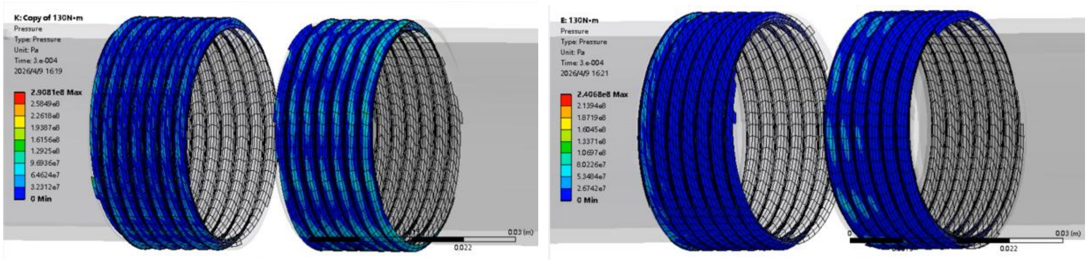

(a) Before Cooling (20 °C) (b) After Cooling (−40 °C)

Figure 2: Contact Pressure Distribution Calculated Using Geometric Rotation Method, 190N·m.

3 Leakage Channel Identification Method Based on the Contact Pressure–Connectivity Criterion

3.1 Limitations of the Original Contact Gap Criterion

In finite element contact analysis of threaded pipe joints, the contact gap is an important parameter for characterizing the local separation state of the contact interface. However, for threaded pairs with complex helical contact characteristics, the numerical value of the gap cannot be directly regarded as the actual effective leakage opening. On the one hand, obvious local warping, variation of contact normal direction, and non-uniform deformation may occur on the thread contact surface during tightening. On the other hand, the gap output from finite element software is also affected by the contact detection algorithm, mesh discretization accuracy, normal projection method, and post-processing interpolation scheme. Therefore, if only the maximum or average gap is used as the sealing performance evaluation index, regions that have already formed effective compacted contact may be incorrectly identified as potential leakage regions.

Torque (N·m)	Thread rotation angle (°)	Average gap before cooling (m)	Maximum gap before cooling (m)	Average gap after cooling (m)	Maximum gap after cooling (m)
40	1	−1.978e−005	−6.7873e−005	−2.8257e−005	−8.2185e−005
70	1.4	−2.1028e−005	−7.1278e−005	−2.8431e−005	−8.4806e−005
100	1.8	−2.2379e−005	−7.4764e−005	−2.879e−005	−8.7801e−005
130	2.2	−2.3819e−005	−7.8282e−005	−2.9392e−005	−9.1055e−005
160	2.6	−2.5321e−005	−8.1869e−005	−3.0271e−005	−9.4401e−005
190	3	−2.6872e−005	−8.5562e−005	−3.1362e−005	−9.7799e−005

Table 5: Gap values under geometric rotation loading.

As shown in Table 5, the original gap values do not exhibit a monotonic decrease with increasing tightening torque. This indicates that relying solely on the contact gap is insufficient to accurately characterize the actual leakage risk of the threaded contact interface. For threaded pipe joints, the formation of a leakage channel depends not only on the local gap size, but also on whether the corresponding region is under low contact pressure and whether the low-pressure region can form a continuous through-path from the inner-diameter side to the outer-diameter side along the contact interface. Therefore, it is necessary to further introduce contact pressure and connectivity criteria based on the gap results.

3.2 Contact Pressure–Connectivity Leakage Criterion

To improve the physical rationality of leakage channel identification, this study proposes a leakage channel identification method based on a contact pressure–connectivity criterion. In this method, the contact pressure, contact gap, contact status, and penetration on the threaded contact interface are first extracted from the finite element results. The contact interface is then divided into effectively compacted regions and candidate leakage regions according to a contact pressure threshold.

In this study, the critical contact pressure is set to \$5 \times 10^7\$ Pa. When the local contact pressure is higher than this critical value, the region is considered to have formed effective compacted contact, which can block the penetration of microscopic gaps; therefore, its equivalent leakage gap is set to zero. When the local contact pressure is lower than the critical value, the region is regarded as insufficiently compacted, and its gap contribution to leakage capacity is retained. Such regions are defined as candidate leakage regions.

After identifying the candidate leakage regions, a connectivity analysis is further conducted on the low-pressure regions. If the candidate leakage regions are only locally and discretely distributed and do not form a continuous path from the inner-diameter side to the outer-diameter side, they are considered insufficient to constitute an effective leakage channel. In contrast, if the candidate leakage regions form a continuous through-path along the threaded contact interface, the path is identified as a potential leakage channel. In this way, the leakage judgment is transformed from a traditional local gap-based evaluation into a spatial connectivity problem, namely whether the low-pressure regions are connected through the interface.

3.3 Leakage Capacity Evaluation Indices

To further compare the leakage risk of threaded pipe joints under different operating conditions, several quantitative indices are introduced based on the identified through-leakage paths, including the number of leakage elements, average gap value, equivalent leakage area, and equivalent flow index.

First, the contact pressure distribution $p_c(x)$ on the threaded contact surface is extracted from the finite element results. Considering that the contact pressure can reflect the compaction degree of the interface, a critical contact pressure p_{cr} is defined to divide the contact surface into two types of regions:

$$\begin{cases} p_c(x) \geq p_{cr}, & compactedregion \\ p_c(x) < p_{cr}, & insufficientlycompactedregion \end{cases} \tag{1}$$

The compacted region represents the area where the contact surface has a relatively high normal contact stress and can effectively suppress the penetration of microscopic gaps. The insufficiently compacted region may contain continuous micro-channels and is therefore regarded as the main carrier of potential leakage paths.

Based on this classification, a connectivity criterion is introduced. If a continuous path composed of insufficiently compacted regions exists on the threaded contact interface and extends from the high-pressure side to the low-pressure side, the path is identified as a potential leakage channel. Conversely, if the path is interrupted by compacted regions, the sealing path is considered blocked. The number of leakage elements is used to characterize the scale of the candidate leakage region. The average gap value reflects the mean opening level of the candidate leakage region. The equivalent leakage area is used to characterize the spatial extent of the through-leakage channel. The equivalent flow index is used to evaluate the relative leakage capacity under different operating conditions.

The equivalent gap height h_{eq} is calculated by taking the cubic average of the gap heights of all nodes along the leakage path and then taking the cubic root:

$$\mathrm{h_{eq}} = \left(\frac{1}{\mathrm{N}}\sum_{\mathrm{i=1}}^{\mathrm{N}} \mathrm{h_i^3}\right)^{1/3} \tag{2}$$

where $h_i = |\mathrm{gap}_i|$, and N is the number of nodes along the leakage path.

The total leakage capacity Q_{total} is not a strict physical flow rate, but a leakage capacity index proportional to the flow rate. It is mainly used to compare the leakage tendency under different operating conditions. Its expression is:

$$\mathrm{Q_{total}} = \sum_{\mathrm{i=1}}^{\mathrm{N}} \mathrm{h_i^3} \tag{3}$$

where b is the channel width, h is the gap height, μ is the dynamic viscosity, L is the flow path length, and Δp is the pressure difference.

It should be noted that the effective area index A_{eff} is not a strict geometrical area, but rather represents the number of nodes or elements participating in the statistical evaluation of the leakage path. Through these indices, the spatial range of the leakage region, the gap opening degree, and the channel flow capacity can be simultaneously characterized. This avoids the misjudgment that may arise from using only the maximum gap or average gap as the sealing evaluation criterion.

4 Leakage Channel Identification Results

4.1 Effect of Tightening Torque on Leakage Channels

Based on the contact pressure–connectivity criterion, leakage channel identification was performed on the threaded contact surfaces under different tightening torque conditions. The results indicate that tightening torque has a significant influence on the distribution and through-connectivity of leakage regions.

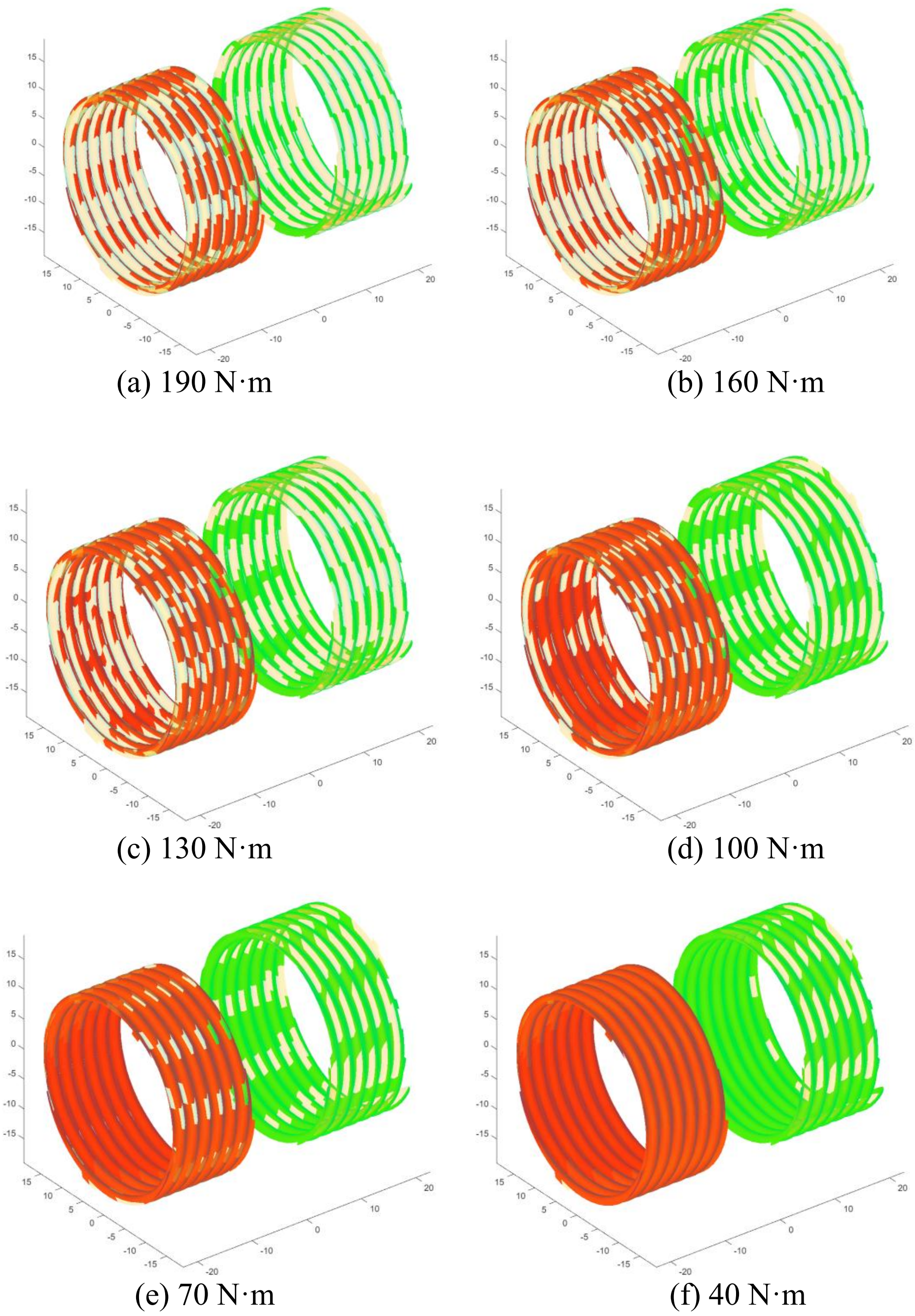

(a) 190 N·m (b) 160 N·m

(c) 130 N·m (d) 100 N·m

(e) 70 N·m (f) 40 N·m

Figure 3: Leakage channel identification results under different tightening torques.

As shown in Figure 3, under low-torque conditions, the high-pressure contact regions on the threaded contact surface are mainly distributed as discrete short strips. The low-pressure regions exhibit strong connectivity in both the circumferential and axial directions, making it easier to form continuous leakage paths from the inner-diameter side to the outer-diameter side.

As the tightening torque increases, the local contact pressure gradually rises, and the area of the high-pressure regions expands with a tendency toward mutual connection. Consequently, the originally continuous low-pressure leakage regions are divided by compacted regions, and the leakage paths gradually change from continuous through-paths to segmented distributions. Under high-torque conditions, the high-pressure contact regions form relatively continuous band-like structures along the thread direction, which effectively block the low-pressure regions and significantly reduce the connectivity of potential leakage channels.

These results demonstrate that increasing the tightening torque can enhance the local compaction between the threaded pair and weaken the through-connectivity of low-pressure leakage channels by enlarging the high-pressure contact regions. However, due to the pronounced non-uniformity of threaded contact, some low-pressure candidate leakage regions may still exist even under relatively high torque. Therefore, a connectivity criterion is still required to determine whether these regions constitute effective leakage channels.

4.2 Effect of Low Temperature on Leakage Channels

To analyze the influence of low-temperature environments on the sealing performance of threaded pipe joints, the leakage channel identification results under 20 °C and −40 °C were compared for each tightening torque. The results show that, after cooling, the candidate leakage regions expand noticeably under all torque conditions. The number of leakage elements, equivalent leakage area, and equivalent flow index are all higher than those under room-temperature conditions, as shown in Figure 4.

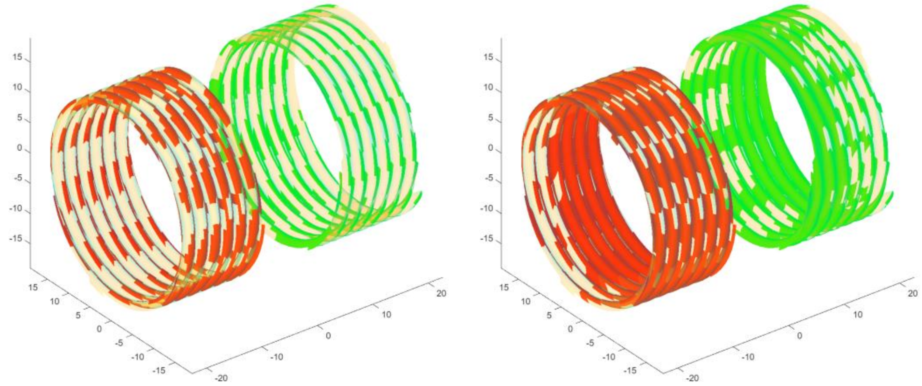

(a) Leakage regions before and after cooling at 190 N·m

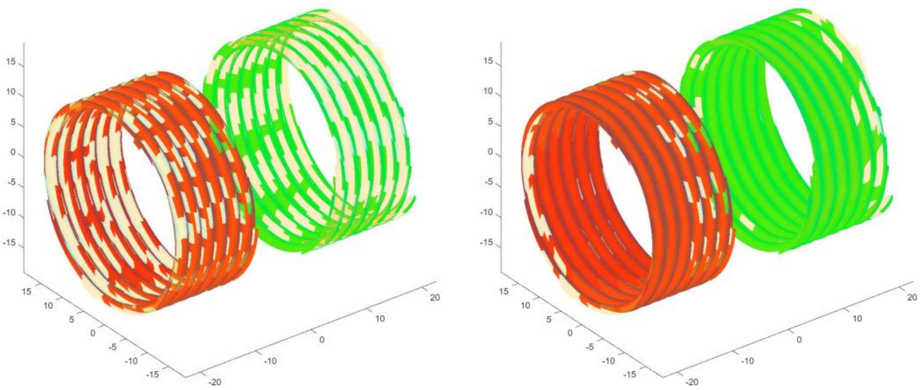

(b) Leakage regions before and after cooling at 130 N·m

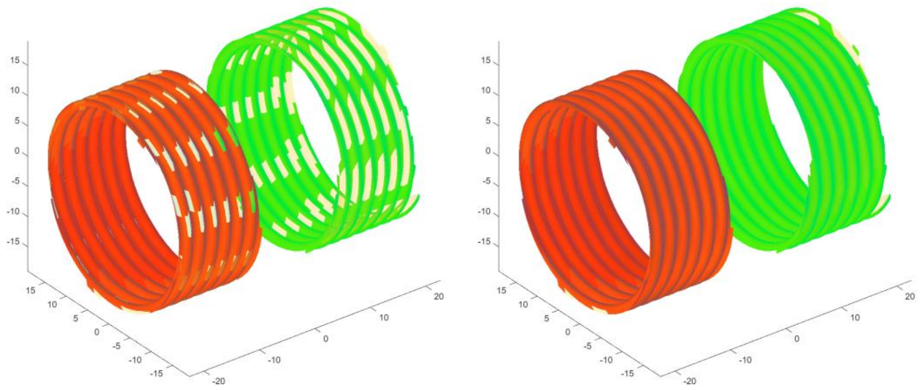

(c) Leakage regions before and after cooling at 70 N·m

Figure 4: Leakage channel identification results before and after cooling under different tightening torques.

As shown in Figure 4, the leakage regions change significantly before and after cooling under different tightening torques. With decreasing temperature, the high-pressure contact regions on the threaded contact surface are reduced, while the connectivity of low-pressure leakage regions increases. These results indicate that low temperature significantly weakens the sealing capability of the threaded contact interface.

This phenomenon can be attributed to the redistribution of the contact state of the threaded pair caused by thermal contraction after cooling. Some regions that were originally in weak contact transform into low-pressure or insufficiently compacted regions, thereby increasing the connectivity of candidate leakage regions on the contact surface.

4.3 Analysis of Equivalent Flow Index and Equivalent Leakage Area

Torque (N·m)	Leakage element number	Average gap	Equivalent flow index (∝ flow rate)	Equivalent leakage area	Change (%)
190	2875	**3.86E-05**	7.40E-11	1282	**291.6**
	5710	**3.98E-05**	**2.16E-10**	3412	
160	3371	3.63E-05	9.26E-11	1930	214.04
	6338	3.83E-05	1.98E-10	3533	
130	4369	3.36E-05	**1.05E-10**	2766	176.57
	6998	3.64E-05	1.85E-10	3837	
100	5634	3.11E-05	9.97E-11	3312	179.07
	7428	3.57E-05	1.79E-10	3928	
70	6468	2.90E-05	8.55E-11	3513	203.77
	7585	3.53E-05	1.74E-10	3959	
40	**7232**	2.71E-05	7.39E-11	**3700**	234.27
	7634	3.52E-05	1.73E-10	**3960**	

Table 6: Equivalent flow index and equivalent leakage area before and after cooling under different tightening torques.

As shown in Table 6, before cooling, the number of leakage elements decreases significantly as the tightening torque increases from 40 N·m to 190 N·m, decreasing from 7232 to 2875. Although the average gap value increases with torque, the equivalent flow index obtained from the comprehensive calculation indicates that, when the torque exceeds 130 N·m, the leakage tendency decreases with increasing torque. This agrees with the general understanding that higher tightening torque improves sealing performance.

However, it should be noted that the similar magnitude of the equivalent flow index under 40 N·m and 190 N·m before cooling does not imply that the sealing performance of the 40 N·m condition is comparable to that of the 190 N·m condition. Further evaluation should be conducted by combining the equivalent flow index with the connectivity criterion and the spatial distribution of leakage channels.

Taking the 190 N·m condition as an example, the number of leakage elements increases from 2875 before cooling to 5710 after cooling. The equivalent leakage area increases from 1282 to 3412, and the equivalent flow index increases from 7.397×10^{-11} to 2.157×10^{-10}, which is approximately 2.92 times the value before cooling. Similarly, for the 160, 130, 100, 70, and 40 N·m conditions, the equivalent flow indices after cooling are approximately 2.14, 1.77, 1.79, 2.04, and 2.34 times those before cooling, respectively.

From the correspondence between experimental observations and numerical results, leakage risk is more likely to increase under low-torque and low-temperature conditions. Although high tightening torque can improve contact pressure and reduce the connectivity of leakage channels, candidate leakage regions may still expand under low-temperature conditions. This trend is generally consistent with the variation of the equivalent flow index obtained from finite element post-processing, indicating that the proposed contact pressure–connectivity criterion can effectively reflect changes in the sealing performance of threaded pipe joints under different assembly and temperature conditions.

5 Conclusions

In this study, a three-dimensional finite element contact model of a conventional threaded pipe joint was established to investigate leakage risk under different tightening torques and low-temperature conditions. A leakage channel identification method based on the contact pressure–connectivity criterion was proposed. The main conclusions are summarized as follows:

(1) The maximum or average gap obtained from finite element analysis is insufficient for evaluating leakage risk in threaded pipe joints. Due to the helical geometry and non-uniform contact characteristics of the threaded interface, gap results may be affected by contact normal direction, mesh discretization, local deformation, and post-processing interpolation. Therefore, contact pressure distribution and low-pressure region connectivity should be considered together.

(2) The proposed contact pressure–connectivity criterion converts leakage evaluation from a local gap-based assessment into a through-channel identification problem. Regions with contact pressure above the critical value are regarded as effectively compacted regions, while continuous low-pressure or insufficiently compacted regions connecting the inner- and outer-diameter sides are identified as potential through-leakage channels.

(3) Increasing tightening torque improves the sealing state of the threaded contact interface. Under low-torque conditions, low-pressure regions are strongly connected in the circumferential and axial directions, making through-leakage paths more likely to form. With increasing torque, high-pressure regions expand and form compacted bands, which interrupt the connectivity of low-pressure channels and reduce leakage risk.

(4) Low temperature weakens the sealing capability of threaded pipe joints. After cooling, the candidate leakage regions expand under all torque conditions, and the leakage element number, equivalent leakage area, and equivalent flow index increase compared with room-temperature conditions. At 190 N·m, the leakage element number increases from 2875 to 5710, the equivalent leakage area increases from 1282 to 3412, and the equivalent flow index increases to approximately 2.92 times its room-temperature value.

(5) Although increasing tightening torque can improve sealing performance, it cannot completely eliminate low-temperature-induced leakage risk. Therefore, tightening parameters, thermal loads, and contact-interface connectivity should be

jointly considered when evaluating and optimizing the sealing reliability of threaded pipe joints in low-temperature service environments.

Acknowledgements

This work was supported by the National Key Research and Development Program of China (2026YFE0103400), Science and Technology Research and Development Programme Topics of China State Railway Group Co., Ltd. (N2022J019), and Shanghai Collaborative Innovation Research Center for Multi-network & Multi-model Rail Transit.

References

[1] W. Chen, Q. Di, H. Zhang, et al., "The Sealing Mechanism of Tubing and Casing Premium Threaded Connections under Complex Loads", Journal of Petroleum Science and Engineering, 171, 724-730, 2018.

[2] Y. Dou, Y. Li, Y. Cao, et al., "FE Simulation of Sealing Ability for Premium Connection Based on ISO 13679 CAL IV Tests", International Journal of Structural Integrity, 12(1), 138-148, 2021.

[3] Y. Liang, "Three-Dimensional Finite Element Analysis and Sealing Performance Study of Premium Threaded Connections for Oil Country Tubular Goods", PhD thesis, Huazhong University of Science and Technology, Wuhan, China, 2023.

[4] B. Yang, H. Xu, S. Xiang, et al., "Effects of Make-Up Torque on the Sealability of Sphere-Type Premium Connection for Tubing and Casing Strings", Processes, 11(1), 256, 2023.

[5] R. Wang, J. Liu, X. Ding, "Quantitative Evaluation and Influence Law of Sealing Performance of Conical Pipe Joints", Transactions of Beijing Institute of Technology, 45(3), 256-264, 2025.

[6] Z. Yang, J. Li, J. Zhu, et al., "Sealing Performance of 60° Spherical Head Conical Pipe Connectors", Journal of Aerospace Power, 40(8), 234-244, 2025.

[7] Y. Yuan, J. Han, G. Zhang, et al., "Finite Element Analysis of Thread Sealing Performance of Double-Ferrule Joints Based on ANSYS", Journal of Liaoning Petrochemical University, 44(5), 82-89, 2024.

[8] W. Yu, "Analysis and Detection Method of the Influence of Assembly Stress on the Sealing Performance of Aircraft Pipelines", PhD thesis, Nanjing University of Aeronautics and Astronautics, Nanjing, China, 2019.

[9] [9] T. Huang, Y. Wu, C. Shi, et al., "Analysis and Optimization for the Sealing Performance of Ultra-High Pressure Solenoid Valves in Low-Temperature Environments", Applied Sciences, 15(17), 9608, 2025.

[10] L. Yang, M. Liu, Y. Liu, et al., "Thermo-Mechanical Coupling Analysis of the Sealing Structure Stress of LNG Cryogenic Hose Fittings", Journal of Marine Science and Engineering, 12(4), 581, 2024.

[11] J. Wang, J. Li, N. Bauer, et al., "Numerical Study of Leakage Rate in Reciprocating Seal with Non-Gaussian Topography Characteristics Using Percolation Mechanism", Tribology International, 199, 109955, 2024.

[12] H. Xu, Z. Zhang, S. Xiang, et al., "Leakage Model of Tubing and Casing Premium Connection Based on Sinusoidal Contact Simulation between Rough Surfaces", Processes, 11(2), 570, 2023.
[13] R. Wang, J. Liu, F. Zhang, et al., "An Approach to Evaluate the Sealing Performance of Sealing Structures Based on Multiscale Contact Analyses", Journal of Computational Design and Engineering, 8(6), 1433-1445, 2021.
[14] F.J. Fischer, K. Schmitz, A. Tiwari, et al., "Fluid Leakage in Metallic Seals", Tribology Letters, 68(4), 125, 2020.